OPEN ACCESS Freely available online

PLOS ONE

Beat-to-Beat Cycle Length Variability of Spontaneously Beating Guinea Pig Sinoatrial Cells: Relative Contributions of the Membrane and Calcium Clocks

Massimiliano Zaniboni[1,2]*, Francesca Cacciani[1], Robert L. Lux[3]

1 Department of Life Sciences, University of Parma, Parma, Italy, **2** Center of Excellence for Toxicological Research, University of Parma, Parma, Italy, **3** Cardiovascular Research and Training Institute, University of Utah, Salt Lake City, Utah, United States of America

Abstract

The heartbeat arises rhythmically in the sino-atrial node (SAN) and then spreads regularly throughout the heart. The molecular mechanism underlying SAN rhythm has been attributed by recent studies to the interplay between two clocks, one involving the hyperpolarization activated cation current I_f (the membrane clock), and the second attributable to activation of the electrogenic NaCa exchanger by spontaneous sarcoplasmic releases of calcium (the calcium clock). Both mechanisms contain, in principle, sources of beat-to-beat cycle length variability, which can determine the intrinsic variability of SAN firing and, in turn, contribute to the heart rate variability. In this work we have recorded long sequences of action potentials from patch clamped guinea pig SAN cells (SANCs) perfused, in turn, with normal Tyrode solution, with the I_f inhibitor ivabradine (3 μM), then back to normal Tyrode, and again with the ryanodine channels inhibitor ryanodine (3 μM). We have found that, together with the expected increase in beating cycle length (+25%), the application of ivabradine brought about a significant and dramatic increase in beat-to-beat cycle length variability (+50%). Despite the similar effect on firing rate, ryanodine did not modify significantly beat-to-beat cycle length variability. Acetylcholine was also applied and led to a 131% increase of beating cycle length, with only a 70% increase in beat-to-beat cycle length variability. We conclude that the main source of inter-beat variability of SANCs firing rate is related to the mechanism of the calcium clock, whereas the membrane clock seems to act in stabilizing rate. Accordingly, when the membrane clock is silenced by application of ivabradine, stochastic variations of the calcium clock are free to make SANCs beating rhythm more variable.

Citation: Zaniboni M, Cacciani F, Lux RL (2014) Beat-to-Beat Cycle Length Variability of Spontaneously Beating Guinea Pig Sinoatrial Cells: Relative Contributions of the Membrane and Calcium Clocks. PLoS ONE 9(6): e100242. doi:10.1371/journal.pone.0100242

Editor: Marcello Rota, Brigham & Women's Hospital - Harvard Medical School, United States of America

Received January 15, 2014; **Accepted** May 23, 2014; **Published** June 18, 2014

Funding: This work has been funded to the corresponding author by Chiesi Farmaceutici S.p.A. within the project "Pharmacological modulation of electrophysiological properties of guinea pig SA nodal cells" 2012–2013. The funders had no role in study design, data collection and analysis, decision to publish, or preparation of the manuscript.

Competing Interests: The fact that the authors received funding from a commercial source (Chiesi Farmaceutici S.p.A) does not alter the authors' adherence to PLOS ONE policies on sharing data and materials.

* E-mail: massimiliano.zaniboni@unipr.it

Introduction

The spontaneous beating activity of the heart is characterized by cycle length variability between consecutive beats, the so called heart rate variability (HRV), which is under primary control of the autonomic nervous system [1]. The complexity related to HRV is required for proper functioning of the cardiac pump, and a wide spectrum of pathological conditions arises when such complexity is lost [2–6]. A certain degree of beat-to-beat variability in the rate of firing is intrinsically present not only at the level of isolated (Langendorff perfused) heart [7], but also within the isolated sino-atrial node (SAN), the natural cardiac pacemaker [8], and even at the level of single cells enzymatically isolated from SAN [6,9,10]. Although it is known that this latter form of variability is modulated by electrotonic interaction within the surrounding tissue [11–13], nonetheless it is relevant to measure it in the various species, since it has been suggested that, in the setting of cardiac disease, a partial breakdown of autonomic control may unmask such intrinsic cellular component of HRV [14].

A first account of the extent of the intrinsic irregularity in the beating rate of single pacemaker heart cells was provided by Wilders and Jongsma [9], who measured a 2.0% coefficient of variability for their inter-beat interval (i.e. cycle length CL). HRV in adult unrestrained rabbits is about 10% [15]. Similar findings are also available for different preparations, including those in spontaneously beating clusters of embryonic chick ventricular cells, single neonatal atrial and ventricular cells, and small groups of neonatal rat heart cells [11,12]. Using computer simulations, Wilders and Jongsma [9] demonstrated that beat-to-beat variability of CL in rabbit SANCs can be well described in terms of stochastic open-close kinetics of membrane ion channels. They also showed that inter-beat variability of CL in isolated SANCs tends to be normally distributed, and that consecutive CLs do not correlate over a lag of 1–20 beats. Furthermore, as pointed out by Rocchetti et al. in isolated rabbit SANCs exposed to ACh or isoproterenol, CL variability is expected to increase with mean CL, simply due to the hyperbolic-like relationship between CL and diastolic depolarization rate [16,17]. Since the main mechanism underlying SAN automaticity has been historically recognized to

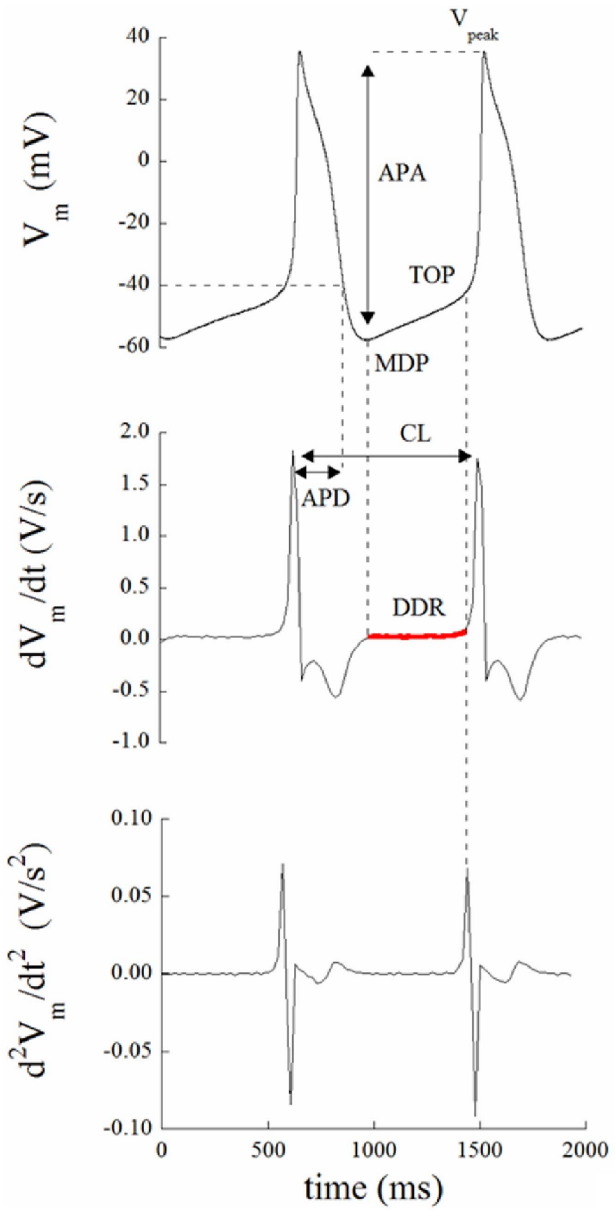

Figure 1. Action potential parameters measurement. Shown are APs (top), first and second time derivatives (middle and bottom, respectively). For each beat, the following parameters were automatically measured: MDP (maximum diastolic potential, mV), as the most negatively polarized value reached by membrane potential during each cycle; V_{peak} (mV), as the most positively polarized value reached by membrane potential during each cycle; APA (action potential amplitude, mV), as the difference between the two preceding parameters; TOP (take-off potential, mV), as the V_m taken at the time of the peak of the second derivative of V_m with respect to time; DD (diastolic depolarization phase, ms), as the time interval between MDP and TOP; DDR (diastolic depolarization rate, V/s), as the average value of the first derivative of V_m over DD (marked in red in the middle panel); APD (action potential duration, ms), as the time between the peak of the first derivative of V_m and the time when V_m reaches the value of −40 mV.
doi:10.1371/journal.pone.0100242.g001

be the hyperpolarization activated I_f current [18–22], it is straightforward to think this current to be involved in the mechanism underlying inter-beat CL variability, and to view it as a possible target for modulating such variability.

Recently, it has been proposed that, in addition to I_f serving as a so-called "membrane clock", rhythmic release of SR calcium also contributes, as a "calcium clock", to SA nodal diastolic depolarization (DD) [23]. The Ca^{2+} clock mechanism operates by generating spontaneous local subsarcolemmal Ca^{2+} releases (LCRs) during late DD, which activate forward Na^+-Ca^{2+} exchange, providing a cyclic source of depolarizing current [24–26]. The stability and flexibility of pacemaker function likely depends on the synergistic interplay between the two clocks [23]. Since the very nature of LCRs that sustain the calcium clock is stochastic, it has been shown recently that their beat-to-beat variations sustain spontaneous beat-to-beat variability of CL in single SANCs [10].

Despite their relevance, the relative roles of both clocks in determining intrinsic beat-to-beat variability of SANCs firing has never been dissected in detail. In the present study we measured beat-to-beat CL variability in sequences of spontaneous action potentials (APs) recorded from enzymatically isolated guinea pig SANCs. We measured the same parameter during pharmacological interventions which were expected to inhibit, in turn, the two clocks, i.e. by exposing the cells to ivabradine, a specific I_f blocker, and to ryanodine, a specific SR release blocker. Our results suggest for the first time that the calcium clock provides a major contribution to beat-to-beat CL variability, as compared to the membrane clock, which is extremely relevant for understanding both the physiology and pharmacology of sinus rhythm.

Materials and Methods

Cell Isolation

Ethics Statement. The experimental procedure was approved by the Veterinary Animal Care and Use Committee of the University of Parma (Prot. N° 41/11) and carried out in strict accordance with the National Ethical Guidelines (Italian Ministry of Health; D.L. vol. 116, January 27, 1992).

The isolation protocol was adapted from [20]. Male Dunkin-Hartley guinea pigs, weighing 300–350 g, were anesthetized by ether inhalation and killed by decapitation. The heart was quickly removed and placed in a beaker containing 60 mL of solution 1 containing 500U heparin, rinsed in the same solution in order to remove blood, and pinned, exposing the anterior ventral face, to the silicon bottom of a plexiglass chamber filled with solution 1 at 35°C (for solutions composition, see below). After removing the ventricles, the anterior wall of the right atrium was split and the posterior wall exposed in order to identify the SAN region, which was then dissected and minced in tiny fragments. These were then transferred into a beaker with solution 1 at 35°C, and gassed with oxygen 100% for 50 minutes. They were then washed in solution 2 and underwent enzymatic digestion in solution 2 containing 2 mg/ml Type I Collagenase (Worthington, Lakewood, NJ, USA), 0.1 mg/ml Elastase (Sigma-Aldrich, Milan, Italy) and 1 mg/ml Albumin for 25 minutes. After a second passage in solution 2 without enzymes, tissue underwent a further phase (15 min) of mechanical dispersion in solution 3.

Calcium concentration was then increased from 0 to 0.8 mM in a 4-step (9 min) process by addition of increasing volumes of solution 1. Cells were then allowed to settle for about 30 minutes, after which supernatant was removed and replaced with solution 1. Cells where used for electrophysiological measurements within the next 6–8 hours.

Solutions

Solution 1: (in mM): NaCl 140; KCl 5.4; $MgCl_2$ 1; $CaCl_2$ 1.8; Glucose 10; HEPES 5; pH 7.4 with NaOH. Solution 2: NaCl 140;

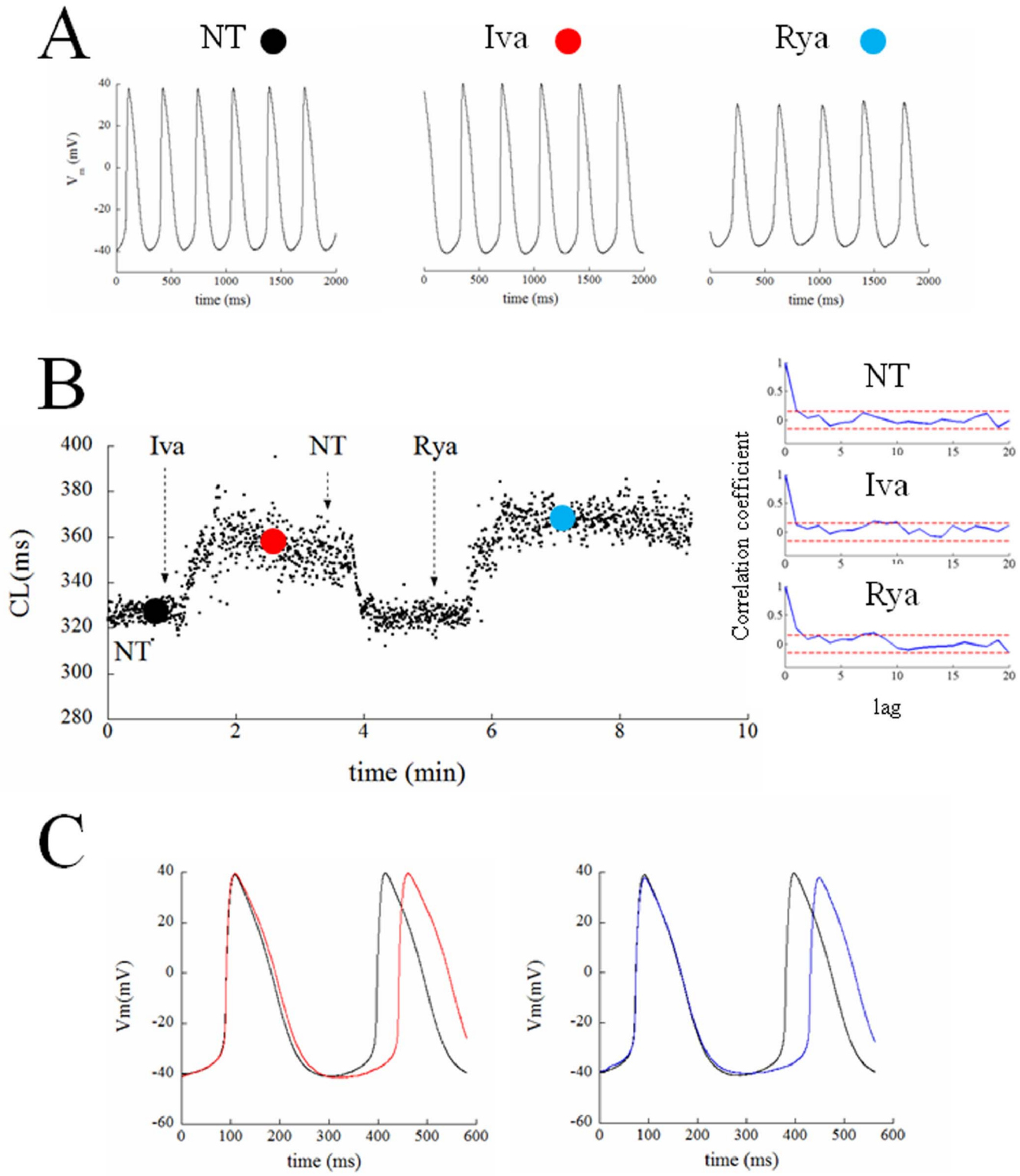

Figure 2. Chronotropic effect of ivabradine and ryanodine. Panel A: Series of APs were recorded from a patch clamped SANC, first perfused in NT, then in 3 μM ivabradine, then back in NT (not shown), and finally in 3 μM ryanodine. Switching times are reported as vertical arrows. Time was allowed for AP parameters to reach the steady state in each perfusion condition, and 2 s samples of each sequence were taken and reported here. Panel B: The time course of CL of the entire experiment is reported on the left. Colored dots represent the times when the 2 s sequences of Panel A were taken. Three sequences of 158 beats were taken from the three regions ending with the colored dots, and underwent autocorrelation analysis of lags of 1–20 beats; results are shown in right Panel. C: Representative examples of the observed bradycardic effect of ivabradine (left) and ryanodine (right) on APs (black: controls; red: ivabradine; blue: ryanodine).
doi:10.1371/journal.pone.0100242.g002

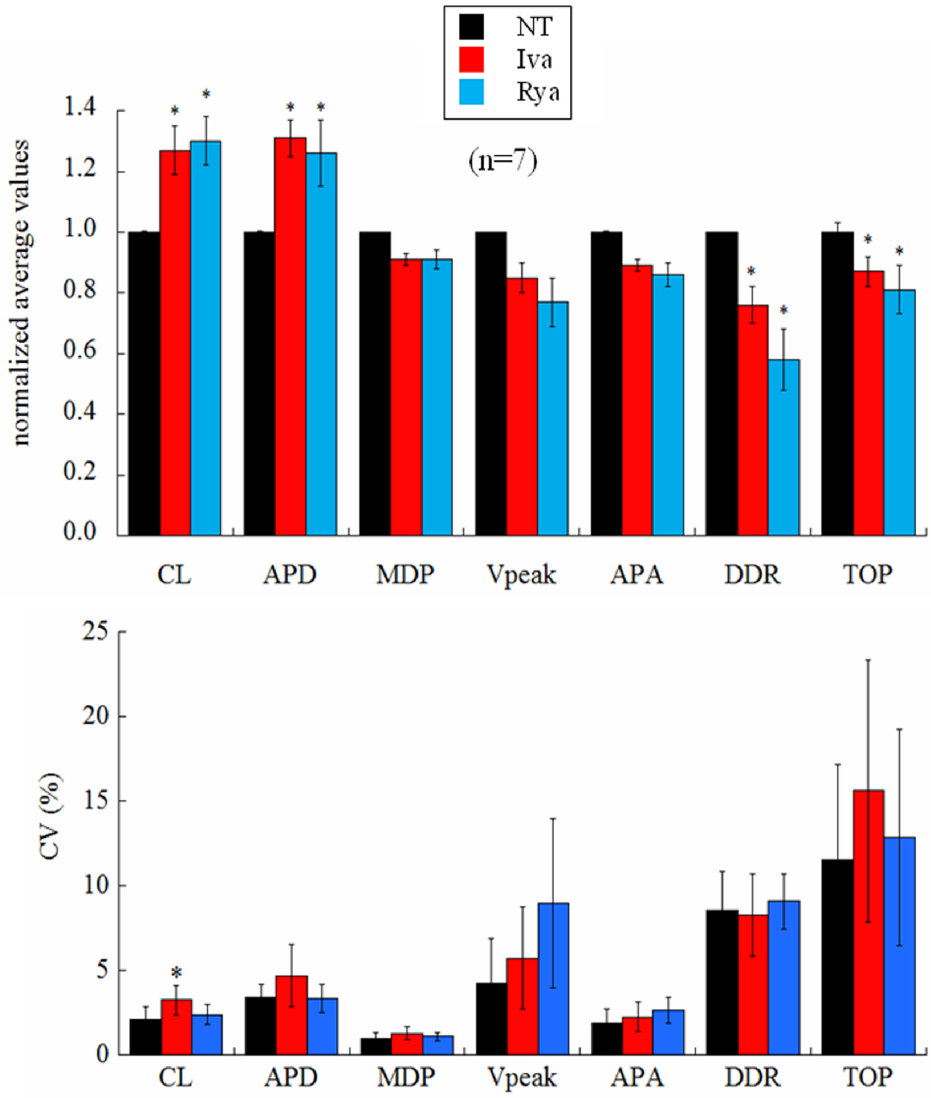

Figure 3. Effects of ivabradine and ryanodine on AP parameters. (Top) The histogram summarizes changes induced on AP parameters by ivabradine (red) and ryanodine (blue) over 30 s sequences after beating reached steady state conditions. All values are reported as normalized with the corresponding mean value measured in NT (black). (Bottom) Corresponding percent changes in beat-to-beat variability of AP parameters, measured as CV. Statistics: paired t-test $p<0.05$ (*).
doi:10.1371/journal.pone.0100242.g003

Table 1. Summary of the effect of Iva and Rya on AP parameters.

	NT	Iva	Rya
CL (ms)	456.6±40.4	578.4±82.3	587.5±76.9
APD (ms)	164.5±7.2	219.6±24.5	211.5±20.0
MDP (mV)	−49.6±3.5	−45.9±4.3	−46.2±4.2
V_{peak} (mV)	29.6±2.7	26.1±4.2	23.3±4.4
APA (mV)	79.4±4.8	72.0±7.6	69.6±6.6
DDR (V/s)	0.09±0.02	0.07±0.02	0.06±0.02
TOP (mV)	−26.0±5.0	−23.2±5.6	−22.8±5.1

The actual mean values (n = 7) of AP parameters following application of Iva and Rya are reported, together with parameter values measured in NT. The same measurements, normalized to NT values, are shown in Figure 3.
doi:10.1371/journal.pone.0100242.t001

KCl 5.4; $MgCl_2$ 0.5; KH_2PO_4 1.2; Taurine 50; Glucose 10; pH 7 with NaOH. Solution 3: KCl 20; KH_2PO_4 10; Glutamic acid 70; β-Hydroxybutyric acid 10; Taurine 10; Glucose 10; Albumin 1 mg/ml; HEPES 10; pH 7.4 with KOH. Solution 4 (also referred to as normal Tyrode, NT): NaCl 140; KCl 5.4; $MgCl_2$ 1; $CaCl_2$ 1.8; Glucose 10; NaH_2PO4 1; HEPES 5; pH 7.4 with NaOH. Solution 5: NaCl 10; KCl 113; $MgCl_2$ 0.5; Glucose 5.5; NaH_2PO4 1; K_2ATP 5; HEPES 10; pH 7.1 with KOH.

Electrophysiological Measurements

Cells in solution 1 were placed in the perfusion chamber of an inverted microscope (Nikon Eclipse T300), allowed to settle for 10 minutes, and then perfused at 36°C with solution 4. Patch pipettes were made from borosilicate capillaries (Clark capillaries, Harvard Apparatus LTD, Edenbridge, UK) by means of a two-step vertical puller (Narishige PC-10, Narishige, Japan) and had a tip resistance, when filled with solution 5, of 2–5 MΩ. Transmembrane potential (V_m) was recorded by means of an Axoclamp 2B amplifier (Molecular Devices, Sunnyvale, CA) adopting the whole-cell configuration of the patch clamp technique, and digitized at a sampling rate of 10 kHz with a 12-bit A/D converter (Digidata 1200, Molecular Devices, Sunnyvale, CA). Pipette potential was set to zero and tip resistance was compensated by bridge-balance before contacting cell membrane. Spontaneously beating cells were brought in patch-clamp whole-cell configuration, and series of action potentials (AP) recorded via the pCLAMP6 software (Molecular Devices, Sunnyvale, CA), under control conditions (solution 4), until the AP configuration reached a steady-state. Perfusion solution was then rapidly switched, by means of a 6-way electro-valve (Cole-Parmer, General Control, Milan, Italy) to a number of different solutions, and the recording protocol repeated. Test solutions were obtained by adding solution 4, in turn, with: acetylcholine (ACh) 10 nM, isoproterenol (Iso) 100 nM, ivabradine (Iva, Sequoia Research Products Ltd, Pangbourne, UK) 3 μM, or ryanodine (Rya, Ascent Scientific Ltd, Bristol, UK) 3 μM. Perfusion of test solutions could last from 3 to 5 minutes, depending on the time needed to reach a new steady state AP configuration. All solutions were kept at 36°C before and during perfusion.

Data Analysis

Data were analyzed by means of a custom software written by co-author R.L. Lux (ScalDyn) running on an Apple MacBook Pro 2.5 GHz, and of a dedicated software written in Matlab (The MathWors, Inc., USA). Long sequences of spontaneous APs were then analyzed to measure the parameters described in Figure 1. Scaldyn algorithms used first and second least mean squared parabolic estimates of first and second derivatives to detect beats, identify AP fiducials (AP onset, peak and MDP times) from which AP amplitudes, intervals and rates were determined. The program detected beats and allowed stacking and scanning of consecutive beats to visualize intervention-induced changes to AP waveform and CL variation. Mean values of parameters and their coefficient of variability (CV = SD/mean*100) were calculated over 30 s sequences of consecutive beats. Beat-to-beat CL variability was also quantified from Poincarè plots representations of CL sequences as:

$$BVR_{CL} = \sum_{n=1}^{N} \frac{|CL_n - CL_{n-1}|}{N\sqrt{2}}$$

where N is the total number of beats of the sequence, and CL_n the n^{th} element of it [27].

Statistical Analysis

Data are presented as mean ± SE. Paired data Student's t tests were performed in order to assess the effect of blockers. Frequency distributions and autocorrelation analysis were performed in Matlab.

Results

Modulation of Membrane and Calcium Clock

The protocol that we applied to each patch clamped guinea pig SANC is illustrated in Figure 2. All patched cells of this study showed spontaneous regular contractions. After AP waveform stability was reached, spontaneous electrical activity was recorded for about 2 min under perfusion of NT solution; perfusion medium was then rapidly switched to a solution containing the I_f inhibitor ivabradine (Iva, 3 μM) for approximately 3 min, then turned back to NT for 2 min, and then again to a NT combined with the SR release channel inhibitor ryanodine (Rya, 3 μM) for 3 min or more. Both inhibitors, at these concentrations, have been previously used to dissect the contribution of I_f and SR Ca^{2+} release to SANC firing rate [28]. In particular, micromolar concentrations (<10 μM) of ryanodine are known to force ryanodine channels into an open sub-conducting state, which leads to the abolishment of SR Ca^{2+} release and Ca^{2+} transient [29,30]. In some cells the seal was lost before the entire sequence of solutions was applied, some did not recover their initial AP configuration after returning in NT from Iva perfusion, while others spontaneously depolarized throughout the experiment. This resulted in a successful application of the entire protocol to only 7 cells, whose data analysis is reported in Figures 2 to 6. Figure 2A shows three typical AP sequences obtained from the same cell at steady state in control condition (NT), during I_f inhibition (Iva), and during SR release inhibition (Rya). An example of the sequence of measured CL of the spontaneous APs during this experiment is illustrated in left panel B. Panel C shows representative examples on how Iva and Rya (red and blue traces respectively) modified the intrinsic AP shape (black line) of this cell. A number of 158 beats was taken from each treatment right before the switch to the next solution and underwent calculation of serial correlation coefficient of lag 1–20 beats (Panel B on the right). No autocorrelation was found (confidence level 0.05, red dotted horizontal lines in each Panel) in any of the three analyzed conditions. A similar result was found in the remaining 6 cells. The autocorrelation test shows that, at least within a 20 beats range, there are not periodic patterns hidden under the beat-to-beat CL variability.

Figure 3 (top) shows paired statistics for all cells. Iva application (red columns) led to a significant 27% prolongation of CL, 31% APD, a 24% decrease of DDR, and a 13% depolarization of TOP. Rya application (blue bars) led to a significant 30% prolongation of CL, 26% prolongation of APD, a 42% decrease of DDR, and a 19% depolarization of TOP. Actual mean values are reported in Table 1. Bottom panel of the same figure shows corresponding beat-to-beat variability, measured as coefficient of variability CV for each AP parameter.

Beat-to-beat CL Variability

Figure 4 presents another example of the complete protocol described above on a different cell. Ten beats of the three sequences, NT, Iva, Rya, are shown in Panel A_1. The longest and shortest AP cycles from each experimental condition are superimposed in Panel A_2 and the entire corresponding time courses of CLs are given in Panel A_3. Spontaneously beating SANCs show beat-to-beat CL variability that significantly

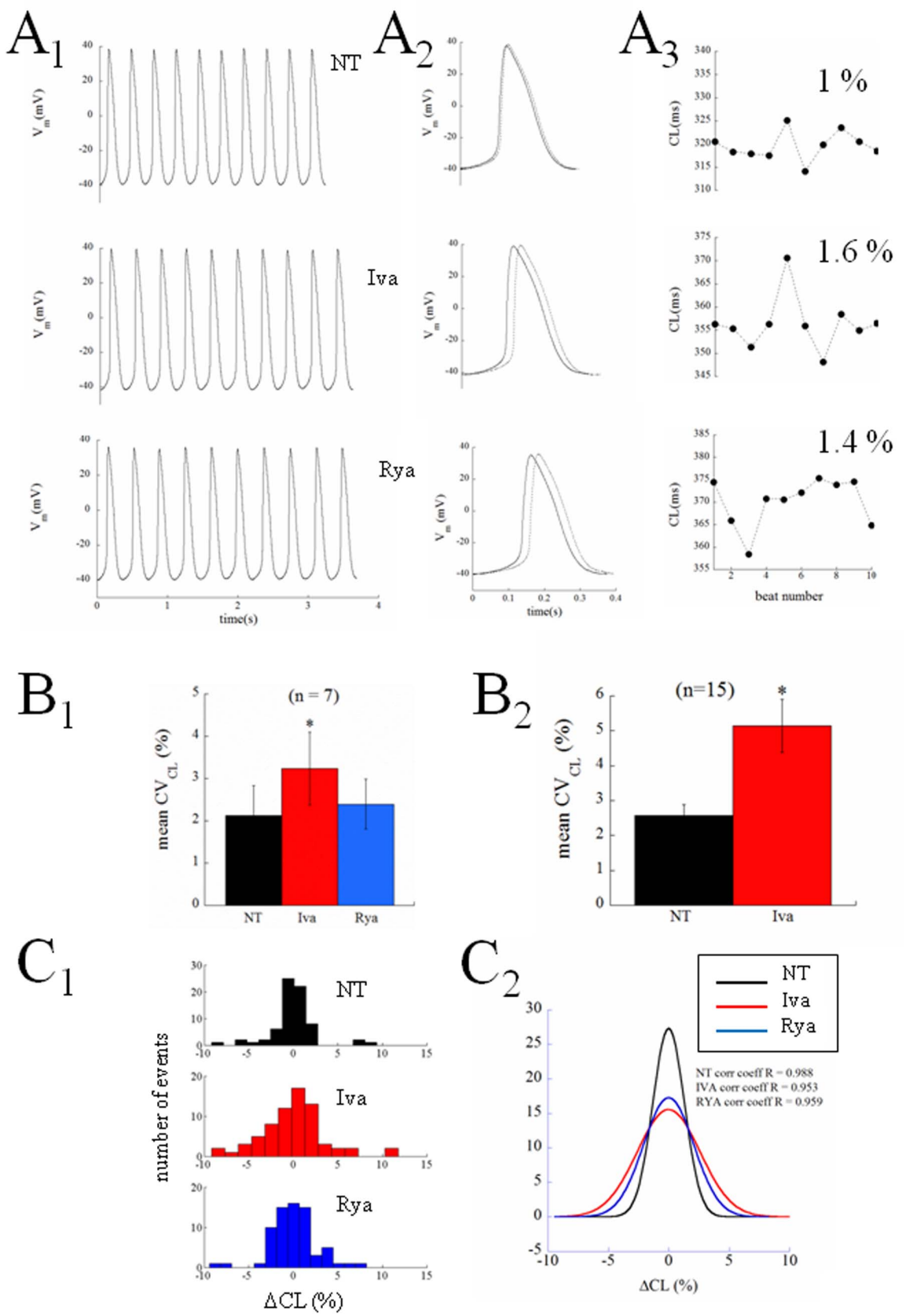

Figure 4. Beat-to-beat variability of CL: percent changes. The same protocol described in Figure 2 was performed on another cell. A_1: 10-beats sequences recorded in the three perfusion conditions. A_2: superimposed shortest (NT) and longest (treated) CLs, referenced to the preceding beat, taken from each sequence. A_3: time course of CL over the corresponding 10 beats. Percent values are CV_{CL} of each 10 beats sequence. B_1: Seven cells

underwent the entire protocol; the average CV_{CL} measured on this sample is reported in the histogram. B_2: On a larger number of cells we only succeeded in applying NT and ivabradine; mean CV_{CL} is reported in the histogram for this larger sample. C_1: all seven 10-beats CL sequences for the 3 perfusion conditions, each one normalized for the corresponding average value of CL, are pooled together in the 15-bins frequency histograms. All frequency distributions were well fitted by Gaussian curves, which are reported in Panel C_2 with the corresponding correlation coefficients. Statistics: paired t-test $p<0.05$ (*).
doi:10.1371/journal.pone.0100242.g004

increased after application of Iva and did not after application of Rya, even though both treatments achieved their expected and similar bradycardic effect. In Panel B_1 we pool together and compare the coefficient of variability (CV_{CL}) measured in 10 beats sequences of the n = 7 cells which underwent the entire protocol. Spontaneously beating SANCs displayed an intrinsic $CV_{CL} = 2.12 \pm 0.71$, this significantly increased up to a value of 3.24 ± 0.86 during exposure to Iva (+52%), and did not undergo significant changes under exposure of Rya (2.39 ± 0.59). As noted above, on several cells we only succeeded in partially applying the protocol; in many cases we could record sequences of APs in NT, in Iva, and, frequently, back in NT, without being able to apply Rya. We can therefore report statistics of the increase of CV_{CL} in Iva on a much larger sample (Panel B_2), and see that, in this case, CV_{CL} changes from the intrinsic 2.58 ± 0.31 up to the value of 5.15 ± 0.76 in Iva (+100%).

Another way to look at these same differences is through the frequency distributions on the three histograms of Panel C_1, where 7x10 beats sequences, each normalized to its average value, were pooled together and reported in 15 bins distributions for NT, Iva, and Rya. Such distributions were well fitted by Gaussian curves, which again show larger dispersion in the case of Iva treatment (Panel C_2). A further proof that the AP sequences analyzed in Figure 4 in terms of CV were indeed at their pacing steady state is provided by the analysis of their Poincarè plots, which is summarized in Figure 5. Beat-to-beat CL variability, when analyzed as BVR_{CL} (see Methods), shows in fact the same qualitative behavior of CV_{CL} (compare Figure 5A and 5C with Figure $4B_1$ and $4C_1$). The absence of relevant asymmetries between the longitudinal and transverse components of Poincarè plots [27,31,16] is evident in the representative example of Figure 5B, which also clearly shows the same bradycardic effect of Iva and Rya, and their quite different effect on inter-beat CL variability. The different degree of beat-to-beat variability of CL is particularly evident in plots like those shown in Figure 6, where the analysis and measurement program, ScalDyn, allows stacking and scrolling through the entire sequence of APs recorded for one cell during the experiment. A common feature of the 7 cells analyzed is that, as already described above and made more clear here, beating rate is very stable under NT perfusion (Panel A), becomes more variable under Iva perfusion (Panels B and C), and doesn't change significantly under Rya perfusion (Panel D). The NT, Iva, and Rya sequences reported in Figure 6 A, C, and D were all taken in steady state AP conditions.

The results presented so far suggest that a much higher degree of stochastic beat-to-beat CL variability is associated with the calcium clock, which is normally damped by the voltage-dependent activation of the membrane clock. Consequently, when the latter is inhibited, CL variability increases. Some smaller stochastic behavior is associated also with the membrane clock, as it is expected also from other ion currents [9,32] underlying SANCs beating. This "control" variability is what is left after inhibiting the calcium clock.

CL Dependency of CL Variability

Previous literature [16] has shown that an increase in CL variability with CL is expected from a simple numerical relationship between AP parameters, which covers control, ACh, and Iso results. In order to verify this relationship within our experimental preparation, we exposed the cells to muscarinic agonist ACh (10 nM) and to the β-adrenergic agonist Iso (100 nM), respectively known to have negative and positive chronotropic effects on spontaneous beating rate of cardiac pacemaker cells (Figure 7). Indeed, Iso led to a significant decrease in average CL (−18%), essentially mediated, among other mechanisms, by a dramatic increase in DDR (+78%), whereas ACh led to a significant increase in average CL (+131%), likely mediated by increase in APD (+7%) and decrease in DDR (−20%). Autocorrelation analysis of the type shown in Figure 2B was also performed on long series of APs under ACh and Iso perfusion and no significant autocorrelation was found in either instance. The Iso-induced modest CL shortening did not lead to any significant change in CV_{CL}, whereas the ACh-induced CL prolongation brought about a 70% increase of CV_{CL} (Figure 7C). Such an increase is slightly larger but within the range documented by Rocchetti et al [16].

In addition to modulating CL with chronotropic agents, we also used hyperpolarizing current injection to slow spontaneous firing. Figure 8A illustrates the results from a spontaneously beating cell subjected to 20 sec of hyperpolarizing current at five different amplitudes (from 10 to 50 pA, step 10). As the cell hyperpolarized, both CL and CV_{CL} increased (panel B). The results from this example are summarized in panel C (black dots), which shows a linear relationship between the average value of CL changes from the last 10 beats of each sequence (shown in detail in Panel B) and the corresponding CV_{CL}. Also included in panel C are results from Rocchetti et al [16] (from figures 2 and 4 of their paper), who found a similar linear relationship between CV_{CL} and ΔCL induced by ACh (green dots for 0, 30, and 40 nM respectively).

Figure 8D summarizes the CV_{CL} versus ΔCL relationship for our results, including control conditions (NT), Rya (blue), ACh (green) and Iva (red). Rya induces a significant increase of CL with a slight (and not statistically significant) increase of CV_{CL}. Similarly, ACh increases CL as well as CV_{CL} up to 4%. Interestingly these changes in CL and CV_{CL}, when considered together with control values (NT, black dot), correlate linearly, as those shown in Panel C. Also, although Iva induces a ΔCL almost identical to that induced by Rya, the corresponding I_f blockade produces an increase in CV_{CL} which is much larger than the one expected from such correlation.

In other words, a certain extent of stochastic electrical noise is likely associated with most of ion channel kinetics throughout DD and is reflected into increase of CL dispersion as DDR decreases, and therefore CL prolongs. While most of whole-cell voltage-dependent ion currents, specifically I_f, are intrinsically deterministic and occasionally stochastic, the calcium clock mechanism is intrinsically stochastic [10]. Accordingly, a fully expressed membrane clock offsets such variability (black dot in Panel D), whereas membrane clock inhibition increases it above the linearly correlating values expected from ion channel kinetics (red dot in the same Panel).

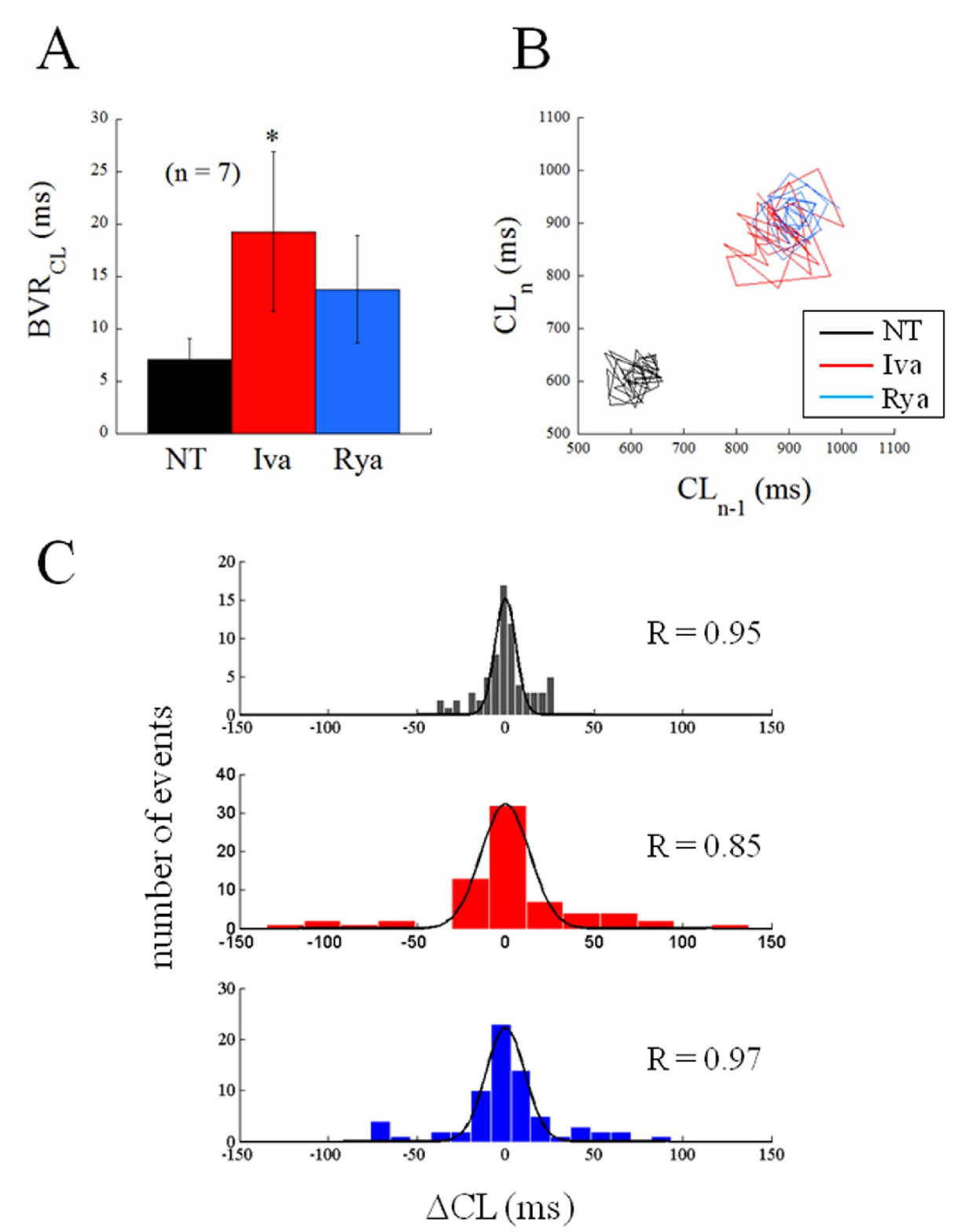

Figure 5. Beat-to-beat variability of CL: absolute changes. The inter-beat variability of the same CL sequences analyzed in Figure 4 in terms of CV (%) were also analyzed in terms of BVR (ms, see Methods). A: average BVR values are reported for the AP sequences recorded in steady state conditions for the 3 different treatments. B: representative example of Poincarè plot for 30 s sequences recorded from the same cell in the 3 experimental conditions after beating rate reached its steady state. C: all seven 10-beats CL sequences for the 3 perfusion conditions reported in panel A were pooled together in the 15-bins frequency histograms. The frequency distributions were well fitted by the superimposed Gaussian curves; fitting correlation coefficients are reported in each panel. Statistics: paired t-test $p<0.05$ (*).
doi:10.1371/journal.pone.0100242.g005

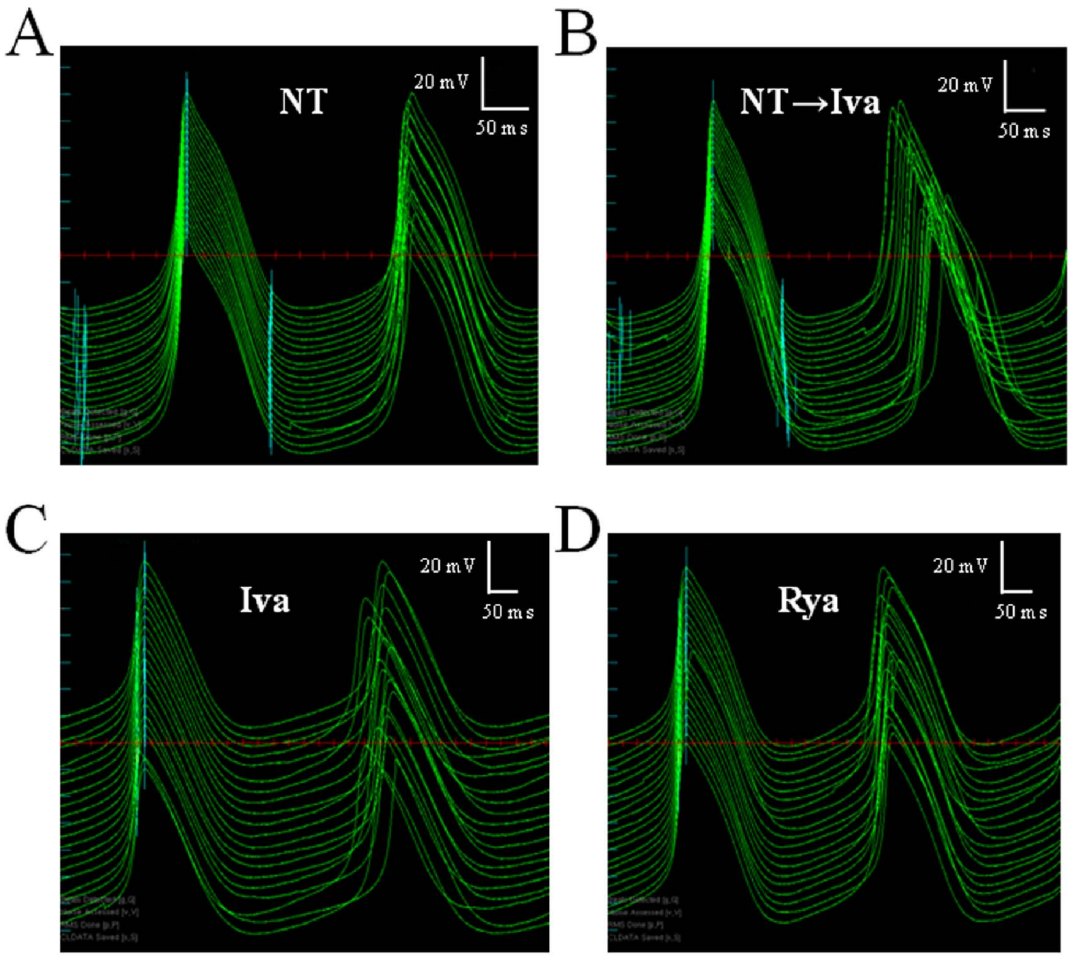

Figure 6. Scrolling through AP sequences with ScalDyn. One of the features of the software ScalDyn is the ability to time-align and stack single, pairs or multiple consecutive APs (with respect to the time of their maximum value of dV_m/dt) of a long sequence, and scroll through the entire recording back and forth. The panels in figure show 20 consecutive pairs of APs recorded from the same cell in different conditions; in each panel APs on the left are synchronized as explained above, whereas those on the right (the succeeding AP for each preceding AP) show average CL changes and beat-to-beat CL variability. Variability in NT is low (A) throughout the entire perfusion time. CL prolongation is evident in B, where APs recorded during the switch between NT and ivabradine are shown (top to bottom). Panel C shows steady state condition with ivabradine displaying the highest level of CL beat-to-beat variability. Steady state condition in ryanodine (D) shows some beat-to-beat variability, though visually much less than in ivabradine.
doi:10.1371/journal.pone.0100242.g006

CL vs DDR Relationship

The non-linear (hyperbolic) relationship between CL and DDR shown by Rocchetti et al. [16] during ACh application to rabbit SANCs holds for all treatments adopted in the present study (see representative examples in Figure 9A and B). When focusing, as we do here, on steady state beating conditions, only a portion of the entire curve is considered, which can always be well fitted with a linear regression (representative examples in Figure 9C and D). The average slope of such regression was found to be (ms^2/mV) −451, −2008, and −1359 for NT, Iva, and Rya perfusion respectively, when measured in all the 7 cells under study (Figure 9E). In order to consider only comparable bradycardic effects, among the 15 cells exposed to ACh, we then selected those (n = 5) whose steady state CL fell within ±2 SD from mean CL in Iva. On these cells, the mean value of the slope of CL vs DDR was −1252 (Figure 9F). These results show that all bradycardic agents lead to an increase in the slope of CL vs DDR, which is much larger in the case of Iva.

Stochastic Events during DD

A useful way to look at the variability of pacing rate is that reported in Figure 10. Panel A illustrates 10 superimposed consecutive APs, each one time-aligned with the preceding MDP, recorded in the three steady state conditions described above, i.e. under perfusion of NT, Iva, and Rya. We then extracted the DD phase of each 10 waveforms, taken from their MDP and TOP respectively (they fall approximately in the grey shaded rectangular area in each Panel of Figure 10A), calculated the average DD trace for each 10-beats sequence, and derived the corresponding difference traces, reported for the three treatments in Panel B. It appears that a certain degree of variation with respect to the average DD is intrinsically present in NT, increases with Iva, and decreases with Rya. This is best seen in the root mean square (RMS) derived for the three different groups of difference-traces and normalized with the time of the CL in NT (Panel C). There is a certain amount of beat-to-beat variation of DD with respect to the average DD in NT, which increases exponentially in proximity of the TOP; overall variation decreases

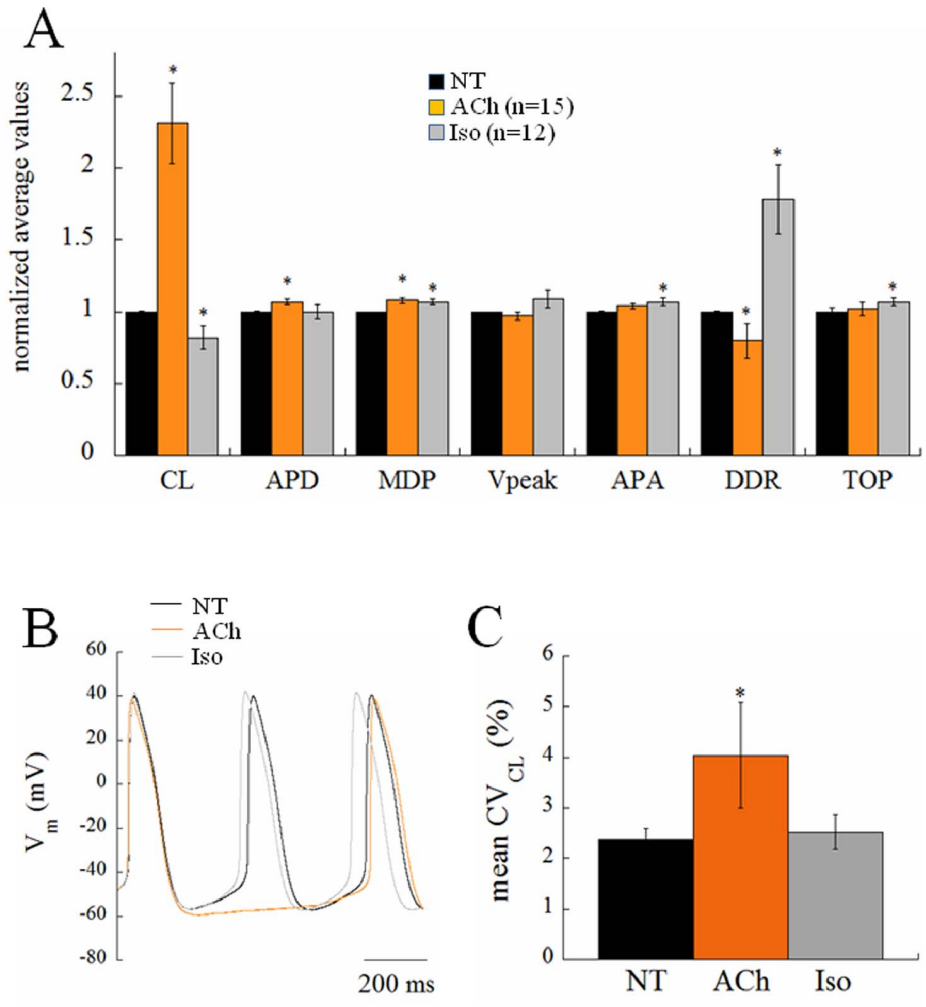

Figure 7. Chronotropic effect of acetylcholine and isoproterenol. Histogram in panel A summarizes the effects of acetylcholine (ACh) and isoproterenol (Iso) on AP parameters. Representative examples of the AP response to both agonists are shown in B. Panel C summarizes changes in beat-to-beat CL variability on a subgroup of n = 8 cells which underwent both treatments sequentially.
doi:10.1371/journal.pone.0100242.g007

during perfusion of Rya and remarkably increases during perfusion with Iva.

The same procedure was performed for the 7 cells and the average values collected in three ranges of DD (from 0 to 10%, from 40 to 50%, and from 70 to 80%, light blue rectangles in Panel C) reported as mean ± SE in Panel D. Whereas the difference between NT and Iva and that between NT and Rya did not always reach the statistical significance, that between Rya and Iva always did so. The cell whose results are reported in Panels A and B was chosen as representative of the overall statistical results of Panel D.

Discussion

The rhythmic spontaneous electrical activity of cardiac SANCs is known to be sustained by two synergistic and coupled mechanisms, one related to the hyperpolarization-induced activation of the membrane ion current I_f (so called 'membrane clock'), the other related to the inward Na^+-Ca^{2+} exchanger current activated by sub-sarcolemmal LCRs (so called 'calcium clock') [23,28]. Also, a long recognized property of SANCs firing is the intrinsic beat-to-beat CL variability of APs that they spontaneously exhibit [9] and that is expected to increase as mean CL does [16,17]. The two clocks have been studied on small aggregates of rabbit SAN cells on the basis of the effects on several AP characteristics during rate modulation by means of Iva, a selective I_f blocker, and of Rya, which inhibits SR calcium release [28]. A clear involvement of the calcium clock in determining intrinsic CL variation of isolated rabbit SAN cells firing has been recently demonstrated [10]. Despite the relevance of the issue, information is still lacking on the relative contribution of the membrane and calcium clock in sustaining and modulating beat-to-beat CL variability of spontaneous APs generated by single SAN cells.

In the present study we specifically addressed this issue in order to test our hypothesis that the calcium clock, being intrinsically stochastic in its mechanism [10], would give a major contribution to beat-to-beat CL variability of SAN cells, as compared to the variability introduced by the membrane clock. In order to test this hypothesis, we patch clamped single guinea pig SANCs in whole-cell configuration, and modulated their firing rate by perfusing them, in turn, with 3 μM Iva, 3 μM Rya, 10 nM ACh, and 100 nM Iso.

The most striking result we found was that, despite the similar (not statistically different) bradycardic effect produced by Iva and

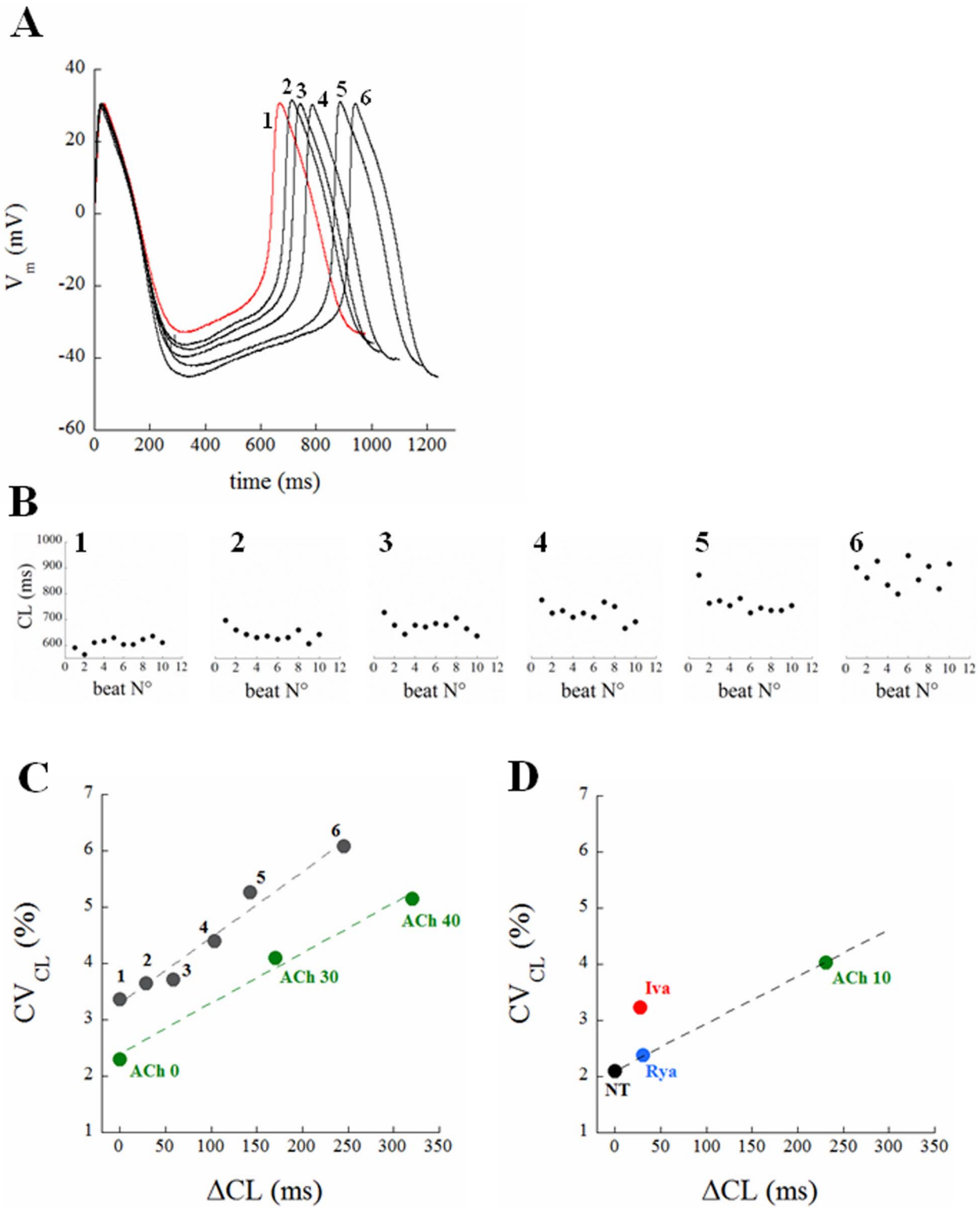

Figure 8. Correlation between CL and CV_{CL}. Panel A: a steady AP waveform from a spontaneously beating single SANC is shown in red (trace 1). The cell was injected with constant hyperpolarizing currents of progressively increasing amplitude, i.e. 0.01, 0.02, 0.03, 0.04, 0.05 nA, each one lasting for 20 s in order to allow AP parameters to reach a new steady state. An AP cycle from the last 10 beats of each 20 s recording was taken and all reported superimposed in panel A (traces 2 to 6). Panel B: time course of CL for the last 10 beats corresponding to each current injection. ΔCL and CV_{CL} values of data in Panel B are summarized in the black dots of Panel C, which are reported together with the linear fit through them. ΔCL with respect to NT and corresponding CV_{CL} at 3 different acetylcholine concentrations (nM) were taken from [16] and also reported in Panel C (green dots). Panel D summarizes results from Figures 4 and 5. The beat-to-beat CL variability associated with each treatment is shown versus the corresponding average induced ΔCL.
doi:10.1371/journal.pone.0100242.g008

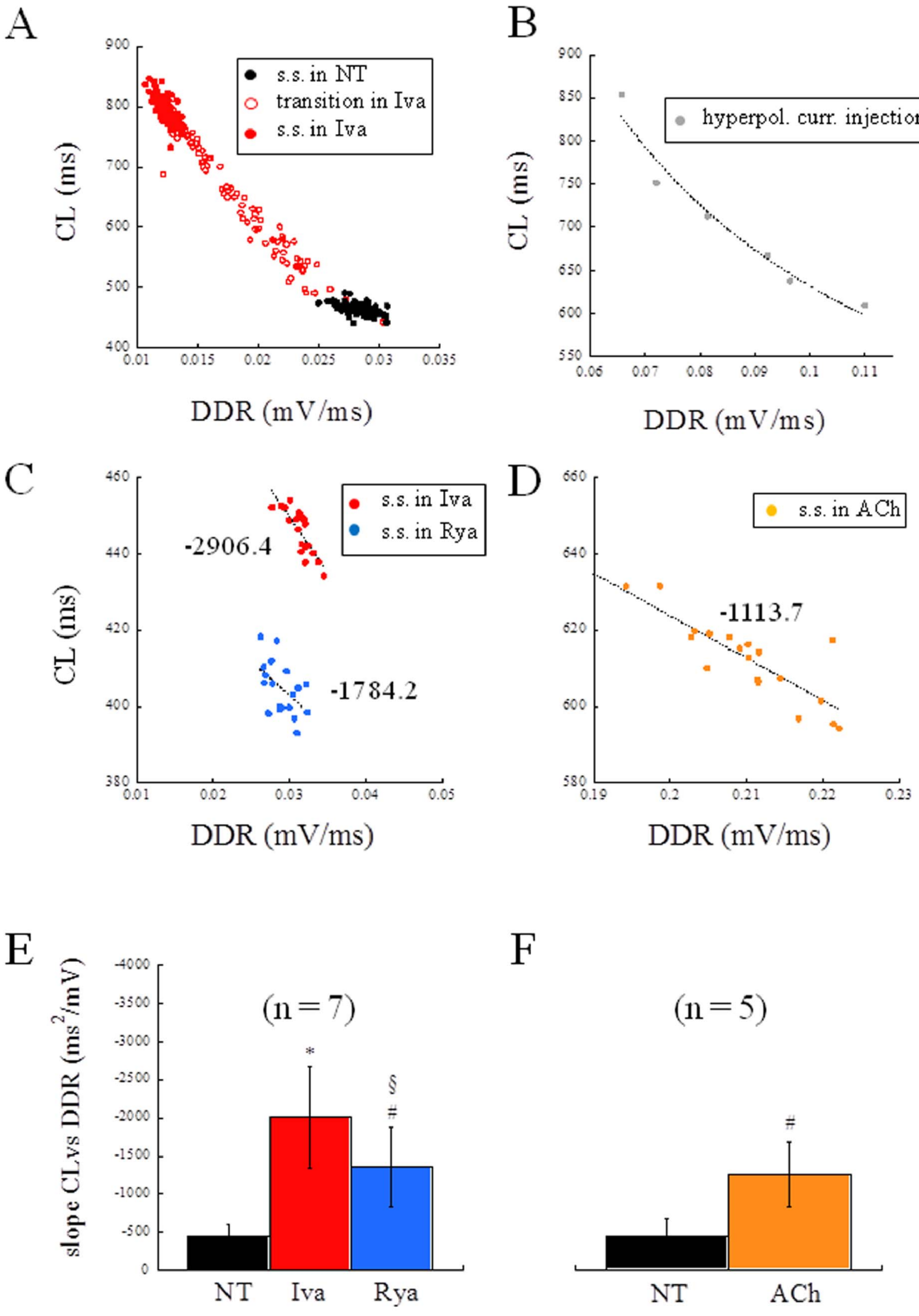

Figure 9. CL vs DDR relationship. Panel A: a representative example of hyperbolic relationship (R = 0.99) between CL vs DDR measured during application of Iva. Black dots refer to beats recorded at the steady state (s.s.) in NT; empty red dots refer to beats recorded right after Iva application; filled red dots refer to beats recorded at the s.s. in Iva. Panel B: CL vs DDR hyperbolic relationship (R = 0.98) measured from APs of the current injection experiment reported in Figure 8A. Panels C and D: steady state CL vs DDR relationships for Iva and Rya (C), and ACh (D) were always well fitted by linear regressions, whose slopes are reported in figure. Panels E and F: the histograms summarize changes induced on the slope of CL vs DDR by Iva and Rya (E) and by ACh (F). Statistics: paired t-test. $p<0.05$ vs NT (*); $p<0.1$ vs NT (#); $p<0.1$ vs Iva (§);
doi:10.1371/journal.pone.0100242.g009

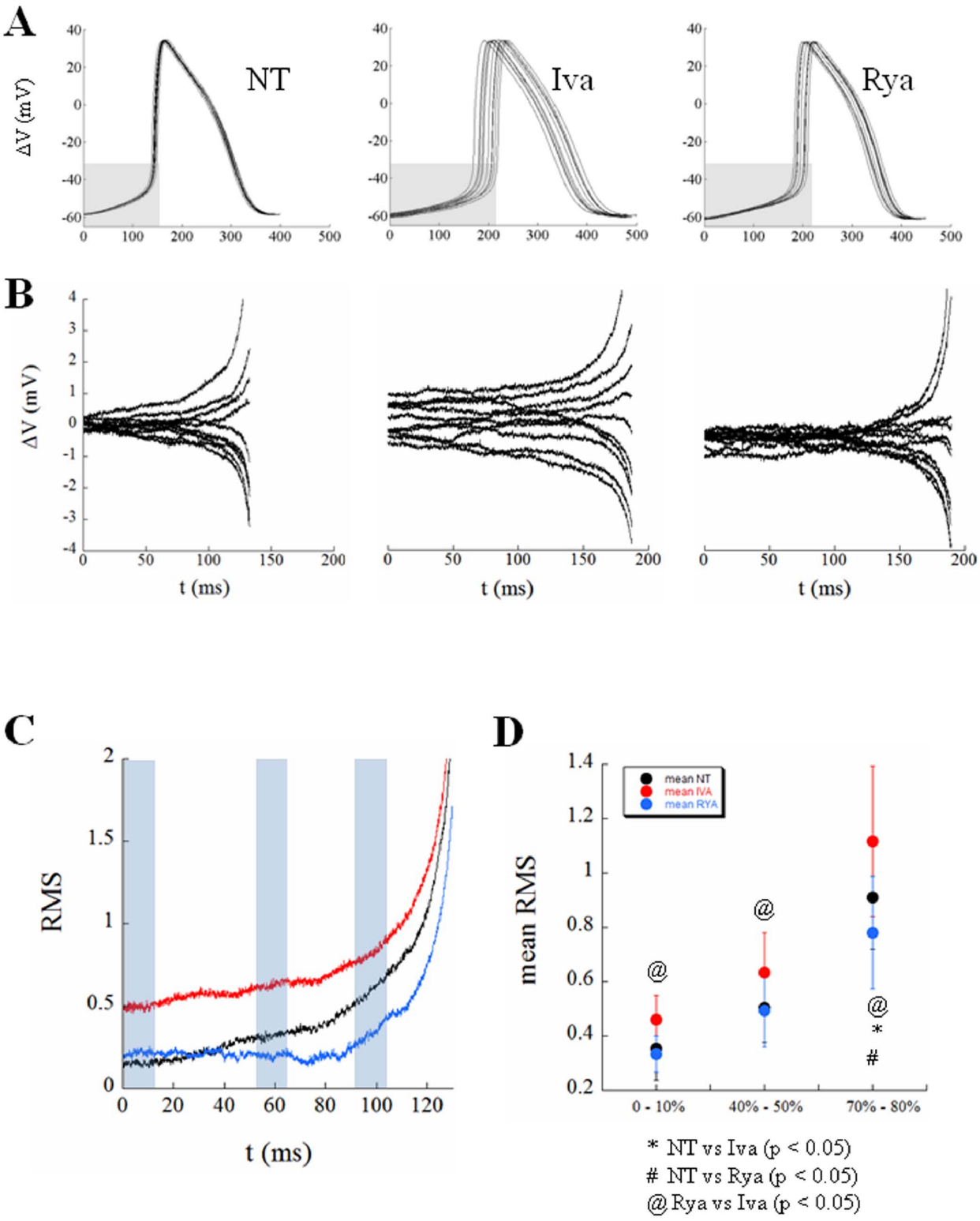

Figure 10. Beat-to-beat noise during DD. Panel A: Ten consecutive APs, time-aligned with the preceding MDP, are reported in each panel from a cell perfused, in turn, with NT, Iva, and Rya. Panel B: The DD phase (from MDP to TOP, corresponding approximately with the grey region in Panels A) was extracted from each curve and the average DD trace calculated for each treatment. The curves measured as the difference between each DD trace and the average DD trace are reported for each treatment. Panel C: The root mean square (RMS) of differences at each time was then calculated for NT (black trace), ivabradine (red), and ryanodine (blue), and all reported normalized to the duration of DD in NT. Panel D: RMSs of differences were then calculated for each one of the 7 cells under study, and the average results summarized for 3 different regions of DD, marked with light blue rectangles in Panel C, and reported in Panel D as mean ± SE.
doi:10.1371/journal.pone.0100242.g010

Rya (~30% increase in CL, cf. with +37% and +16% respectively found by Gao et al. in canine SANCs [33]), the two treatments led to a quite different variation in the level of beat-to-beat CL variability with respect to NT (Figure 3). CV_{CL} was 2.12% in normal conditions (NT), which is comparable to that shown by Wilders and Jongsma in single rabbit SAN cells (2.00%) and by Rocchetti et al. on the same preparation (2.30%) [9,16]. Iva significantly increased CV_{CL} by 52% (by 100% in a larger sample), whereas Rya produced no significant change. The different effect of the two inhibitors on CL variability holds not only for relative changes (CV, %; Figure 4), but also for absolute ones (BVR, ms; Figure 5), despite the rather high dispersion of CL control (NT) values (see Table 1). This strengthens our observation, even in the absence of a significant difference in CL variability between Iva and Rya groups. The negligible presence of a longitudinal (along the bisecting line) component in our CL Poincarè plots (see representative example in Figure 5B) provides a further proof that AP sequences have been recorded in steady state pacing conditions [27,31,34]. Furthermore, all CL time series in NT were normally distributed (Figure 4C) and did not show significant autocorrelation within a lag 1 −20 beats (right Panel of Figure 2B), which also confirms the findings of Wilders and Jongsma in rabbit SAN cells. Both normal correlation and autocorrelation results hold during treatment with Iva and Rya, i.e. beat-to-beat changes in CL are randomly distributed and there is no apparent short-term memory involved in their time evolution, nor any average CL drift within the analyzed AP sequences. Similarly, normal distribution and absence of significant autocorrelation were found during ACh and Iso exposure (data not shown).

Although somewhat expected, changes in beat-to-beat variability of AP parameters other than CL are not strictly required in order to explain the increase in CV_{CL}. From one hand, in fact, the system under study is over-determined with respect to AP trajectory, i.e. a certain phenotype (in our case a given CV_{CL}) may correspond to a number of different parameters combinations [35,36]. On the other hand, TOP depolarization (see top panel of Figure 3), for instance, can lead *per se* to an increase in CV_{CL}, as the same extent of DDR variability can bring about such an increase when a more depolarized TOP has to be reached.

The increase in beat-to-beat CL variability during bradycardic interventions (including hyperpolarizing current injections), was expected from the known hyperbolic CL vs DDR relationship [16]. At slower beating rates, in fact, DDR gets smaller and the slope of CL vs DDR gets steeper, i.e. small changes in DDR lead to large CL changes on a beat-to-beat basis (see for instance Iva application in Figure 9A). When the calcium clock was inhibited, the beating rate slowed, and, following the decrease in mean DDR, the slope of CL vs DDR increased, as during ACh application (Figure 9E and F). The Rya-induced increase in the slope of CL vs DDR though, was not enough to bring about a significant increase in beat-to-beat CL variability. The much larger Iva-induced increase in slope led instead to the larger and significant increase in beat-to-beat CL variability that we document in the present study. This suggests that, when I_f functions as the main clock, the increase in CV_{CL} with CL follows the same law that regulates increase in CL variability during bradycardic interventions like current-induced hyperpolarization or muscarinic activation (Figure 8C and D). On the contrary, when the quasi-deterministic (mainly voltage-dependent) clock associated with whole-cell I_f is turned down, the intrinsic complex mechanism of the calcium clock can express all of its stochastic nature, leading to a significant increase in CV_{CL} (Figure 4 and red dot in Figure 8D) and reinforcing the view of a stabilizing role of I_f on SAN beating rate [37]. These stochastic fluctuations are present, as recently demonstrated [10], already at the very beginning of DD, but persist throughout this phase until the TOP (see Figure 10B, C, and D). A possible role of I_{Kr} inactivation in regulating pacemaker activity has been demonstrated in the past [38,39] and could be involved in the observed Iva- and Rya-dependent APD prolongations. On the other hand, these were not accompanied by significant changes in MDP, nor in beat-to-beat APD variability, which has been shown to follow I_{Kr} inhibition in other cardiac cell types [32,40], ruling out therefore a clear interplay between I_{Kr} and CL variability.

The present study describes for the first time the relative contribution of the two cardiac pacemaker clock mechanisms to the intrinsic variability of SANC beating rate. It would be tempting to explain the higher extent of CL variability induced by Iva application as a consequence of a much relevant decrease in total ionic current flowing through the membrane after I_f blockade. We have recently shown in a simulation study [41] that membrane resistance increases very much during SANCs DD; partial closure of I_f channels would make it even larger and lead therefore to a much higher sensitivity of AP trajectory to stochastic electrogenic LCRs of the calcium clock. We realize that this explanation is, at present, only speculative, and expect that simulations with SANC AP models including both membrane and calcium clocks [42] will better elucidate the mechanism.

Future investigations on more complex preparations, like isolated SA node or Langendorff perfused heart, could further dissect the relative contribution of the two clocks to the rate variability of SAN. The novel information provided here is, on the other hand, relevant in order to better understand the cellular control mechanism of physiological cardiac pacemaker rate, as well as to guide pharmacological research in developing new molecules for the fine regulation of cardiac rhythm and of its variability.

Acknowledgments

We thank Ken Spitzer, from the Nora Eccles Harrison CVRTI, University of Utah, for careful reading and valuable comments during the preparation of the manuscript.

Author Contributions

Conceived and designed the experiments: MZ FC RLL. Performed the experiments: MZ FC. Analyzed the data: MZ FC RLL. Contributed reagents/materials/analysis tools: MZ FC RLL. Wrote the paper: MZ.

References

1. Posokhova E, Ng D, Opel A, Masuho I, Tinker A, et al. (2013) Essential Role of the m2R-RGS6-IKACh Pathway in Controlling Intrinsic Heart Rate Variability. PLoS One 8: e76973.
2. Goldberger AL (1991) Is the normal heartbeat chaotic or homeostatic? News Physiol Sci 6: 87–91.
3. Costa M, Goldberger AL, Peng CK (2005) Broken asymmetry of the human heartbeat: loss of time irreversibility in aging and disease. Phys Rev Lett 95: 198102.
4. Appel ML, Berger RD, Saul JP, Smith JM, Cohen RJ (1989) Beat to beat variability in cardiovascular variables: noise or music? J Am Coll Cardiol 14: 1139–1148.
5. Malik M, Camm AJ (1994) Heart rate variability and clinical cardiology. Br Heart J 71: 3–6.
6. Papaioannou VE, Verkerk AO, Amin AS, de Bakker JM (2013) Intracardiac origin of heart rate variability, pacemaker funny current and their possible association with critical illness. Curr Cardiol Rev 9: 82–96.
7. Frey B, Heger G, Mayer C, Kiegler B, Stöhr H, et al. (1996) Heart rate variability in isolated rabbit hearts. Pacing Clin Electrophysiol 19: 1882–1885.

8. Opthof T, VanGinneken AC, Bouman LN, Jongsma HJ (1987) The intrinsic cycle length in small pieces isolated from the rabbit sinoatrial node. J Mol Cell Cardiol 19: 923–934.
9. Wilders R, Jongsma HJ (1993) Beating irregularity of single pacemaker cells isolated from the rabbit sinoatrial node. Biophys J 65: 2601–2613.
10. Monfredi O, Maltseva LA, Spurgeon HA, Boyett MR, Lakatta EG, et al. (2013) Beat-to-Beat Variation in Periodicity of Local Calcium Releases Contributes to Intrinsic Variations of Spontaneous Cycle Length in Isolated Single Sinoatrial Node Cells. PLoS One 8: e67247.
11. Clay JR, DeHaan RL (1979) Fluctuations in interbeat interval in rhythmic heart-cell clusters. Role of membrane voltage noise. Biophys J 28: 377–389.
12. Jongsma HJ, Tsjernina L, de Bruijne J (1983) The establishment of regular beating in populations of pacemaker heart cells. A study with tissue-cultured rat heart cells. J Mol Cell Cardiol 15: 123–133.
13. Joyner RW, van Capelle FJ (1986) Propagation through electrically coupled cells. How a small SA node drives a large atrium. Biophys J 50: 1157–1164.
14. Kucera JP, Heuschkel MO, Renaud P, Rohr S (2000) Power-law behavior of beat-rate variability in monolayer cultures of neonatal rat ventricular myocytes. Circ Res 86: 1140–1145.
15. Manzo A, Ootaki Y, Ootaki C, Kamohara K, Fukamachi K (2009) Comparative study of heart rate variability between healthy human subjects and healthy dogs, rabbits and calves. Lab Anim43: 41–45.
16. Rocchetti M, Malfatto G, Lombardi F, Zaza A (2000) Role of the input/output relation of sinoatrial myocytes in cholinergic modulation of heart rate variability. J Cardiovasc Electrophysiol 11: 522–530.
17. Zaza A, Lombardi F (2001) Autonomic indexes based on the analysis of heart rate variability: a view from the sinus node. Cardiovasc Res 50: 434–42. Review.
18. Brown HF, DiFrancesco D, Noble SJ (1979) How does adrenaline accelerate the heart? Nature. 1979; 280(5719): 235–236.
19. DiFrancesco D (1985) The cardiac hyperpolarizing-activated current, if. Origins and developments. Prog Biophys Mol Biol 46: 163–183. Review.
20. DiFrancesco D, Ferroni A, Mazzanti M, Tromba C (1986) Properties of the hyperpolarizing-activated current (if) in cells isolated from the rabbit sino-atrial node. J Physiol. 377: 61–88.
21. DiFrancesco D (1991) The contribution of the 'pacemaker' current (if) to generation of spontaneous activity in rabbit sino-atrial node myocytes. J Physiol434: 23–40.
22. DiFrancesco D (1993) Pacemaker mechanisms in cardiac tissue. Annu Rev Physiol. 55: 455–472.
23. Maltsev VA, Lakatta EG (2009) Synergism of coupled subsarcolemmal Ca2+ clocks and sarcolemmal voltage clocks confers robust and flexible pacemaker function in a novel pacemaker cell model. Am J Physiol Heart Circ Physiol 296: H594–615.
24. Rigg L, Terrar DA (1996) Possible role of calcium release from the sarcoplasmic reticulum in pacemaking in guinea-pig sino-atrial node. Exp Physiol 81: 877–880.
25. Hüser J, Blatter LA, Lipsius SL (2000) Intracellular Ca2+ release contributes to automaticity in cat atrial pacemaker cells. J Physiol 524: 415–422.
26. Bogdanov KY, Vinogradova TM, Lakatta EG (2001) Sinoatrial nodal cell ryanodine receptor and Na(+)-Ca(2+) exchanger: molecular partners in pacemaker regulation. Circ Res 88: 1254–1258.
27. Johnson DM, Heijman J, Pollard CE, Valentin JP, Crijns HJ, et al. (2010) I(Ks) restricts excessive beat-to-beat variability of repolarization during beta-adrenergic receptor stimulation. J Mol Cell Cardiol 48: 122–30.
28. Bucchi A, Baruscotti M, Robinson RB, DiFrancesco D (2007) Modulation of rate by autonomic agonists in SAN cells involves changes in diastolic depolarization and the pacemaker current. J Mol Cell Cardiol 43: 39–48.
29. Meissner G (1994) Ryanodine receptor/Ca2+ release channels and their regulation by endogenous effectors. Annu Rev Physiol 56: 485–508. Review.
30. Bucchi A, Baruscotti M, Robinson RB, DiFrancesco D (2003) I(f)-dependent modulation of pacemaker rate mediated by cAMP in the presence of ryanodine in rabbit sino-atrial node cells. J Mol Cell Cardiol 35: 905–13.
31. Korpelainen JT, Sotaniemi KA, Mäkikallio A, Huikuri HV, Myllylä VV (1999) Dynamic behavior of heart rate in ischemic stroke. Stroke 30: 1008–13.
32. Zaniboni M, Pollard AE, Yang L, Spitzer KW (2000) Beat-to-beat repolarization variability in ventricular myocytes and its suppression by electrical coupling. Am J Physiol Heart Circ Physiol 278: H677–87.
33. Gao Z, Chen B, Joiner ML, Wu Y, Guan X, et al. (2010) I(f) and SR Ca(2+) release both contribute to pacemaker activity in canine sinoatrial node cells. J Mol Cell Cardiol 49: 33–40.
34. Schechtman VL, Raetz SL, Harper RK, Garfinkel A, Wilson AJ, et al. (1992) Dynamic analysis of cardiac R-R intervals in normal infants and in infants who subsequently succumbed to the sudden infant death syndrome. Pediatr Res 31: 606–12.
35. Sarkar AX, Sobie EA (2010) Regression analysis for constraining free parameters in electrophysiological models of cardiac cells. PLoS Comput Biol. 2: 6.
36. Zaniboni M, Riva I, Cacciani F, Groppi M (2010) How different two almost identical action potentials can be: a model study on cardiac repolarization. Math Biosci. 228: 56–70.
37. Noble D, Denyer JC, Brown HF, DiFrancesco D (1992) Reciprocal role of the inward currents ib, Na and i(f) in controlling and stabilizing pacemaker frequency of rabbit sino-atrial node cells. Proc Biol Sci 250: 199–207.
38. Song DK, Earm YE, Ho WK (1999) Blockade of the delayed rectifier K+ currents, IKr, in rabbit sinoatrial node cells by external divalent cations. Pflugers Arch. 438: 147–53.
39. Clark RB, Mangoni ME, Lueger A, Couette B, Nargeot J, et al. (2004) A rapidly activating delayed rectifier K+ current regulates pacemaker activity in adult mouse sinoatrial node cells. Am J Physiol Heart Circ Physiol. 286: H1757–66.
40. Spitzer KW, Pollard AE, Yang L, Zaniboni M, Cordeiro JM, et al. (2006) Cell-to-cell electrical interactions during early and late repolarization. J Cardiovasc Electrophysiol 17 Suppl 1:S8–S14. Review.
41. Zaniboni M (2012) Heterogeneity of intrinsic repolarization properties within the human heart: new insights from simulated three-dimensional current surfaces. IEEE Trans Biomed Eng 59: 2372–2380.
42. Severi S, Fantini M, Charawi LA, DiFrancesco D (2012) An updated computational model of rabbit sinoatrial action potential to investigate the mechanisms of heart rate modulation. J Physiol 590: 4483–4499.